

Thermal stabilization of phase and structural state in binary lamellar metallic systems

This article has been downloaded from IOPscience. Please scroll down to see the full text article.

2006 J. Phys.: Condens. Matter 18 4113

(<http://iopscience.iop.org/0953-8984/18/17/001>)

View [the table of contents for this issue](#), or go to the [journal homepage](#) for more

Download details:

IP Address: 129.252.86.83

The article was downloaded on 28/05/2010 at 10:22

Please note that [terms and conditions apply](#).

Thermal stabilization of phase and structural state in binary lamellar metallic systems

K K Kadyrzhanov¹, V S Rusakov² and T E Turkebaev¹

¹ Institute of Nuclear Physics NNC RK, Almaty 480082, Kazakhstan

² Moscow State University, Moscow 119899, Russia

Received 8 September 2005, in final form 23 January 2006

Published 13 April 2006

Online at stacks.iop.org/JPhysCM/18/4113

Abstract

The paper proposes and describes a physical model of thermally induced processes in binary lamellar systems. The model has been developed for the theoretical explanation of an experimentally revealed fact of thermal stabilization of intermetallic phases on the surface of a lamellar sample. Based on the model we developed an algorithm for calculations and a computer code that operates with three one-phase and two two-phase regions in the binary alloy state diagram. The computational model includes as inputs changes in concentration boundaries for existing phases with change in temperature, as well as arbitrary temperature–time regimes for the thermal treatment of the lamellar system under investigation. Good agreement between the theoretical calculations and Mössbauer investigations of binary lamellar Fe–Be systems has been achieved.

1. Introduction

The method of ion-plasma sputtering is widely used for direct modification of metal material surface layers for improvement of the surface properties. Such lamellar materials could be of practical interest only with the formation of thermally stable heterogeneous phase depth distribution.

Based on the proposed thermodynamic approach, in order to achieve an equilibrium spatial heterogeneous phase-structural state [1], experimental and theoretical studies of thermally induced processes of diffusion and phase formation in lamellar metallic systems were performed [2–8]. These investigations made it possible not just to reveal the sequence and characteristic times of phase transformation in subsurface layers and in the bulk; they showed that the direction of such transformation is determined by changes in local component concentrations during their mutual diffusion. These investigations also made it possible to obtain thermal stabilization of the spatially heterogeneous phase-structural state distribution [4, 5].

A physical model [2–4] has been proposed for a quantitative description of thermally induced diffusion and phase formation in the lamellar Fe–Be systems, based on Darken's

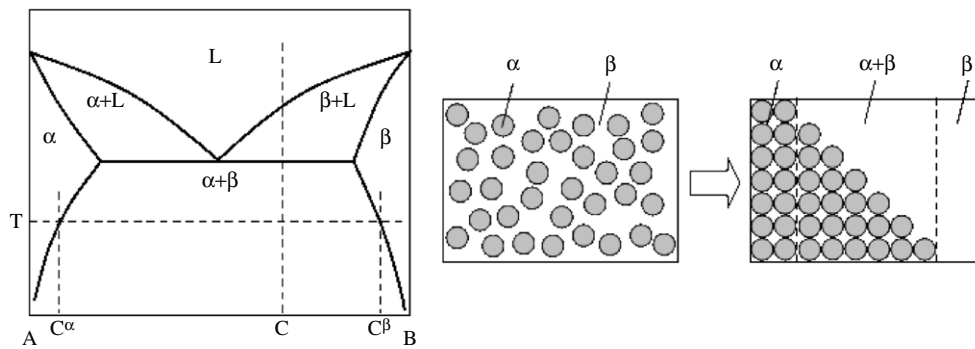


Figure 1. Schematic phase diagram of A–B alloy and possible distribution of α -phase particles over sample depth at thermodynamic equilibrium.

phenomenology theory of mutual diffusion [9, 10] that describes experimental data for Be average bulk concentrations below the solubility threshold for beryllium in α -Fe. However, its framework does not allow an overall description of the observed process of thermal stabilization, because the peculiarities of the diffusion process in two-phase regions of lamellar systems are ignored.

In the present paper, we consider a physical model of thermally induced diffusion and phase formation in binary lamellar metal systems. The model is based on proposed mechanism of mutual diffusion in two-phase concentration regions and describes the process of thermal stabilization of the inhomogeneous phase-structural state.

The main idea of the thermodynamic approach to obtaining the equilibrium spatially heterogeneous phase-structural state [1] is in the determination of the composition and phase-structural state of a sample that provides zero gradients of chemical potential for all the components at a given temperature. Figure 1 presents a schematic equilibrium phase diagram of a simple binary A–B alloy; solutions of both the component A in the component B (β -phase) and B in A (α -phase) are possible. Consider the case when this alloy is heated to temperature T , with chemical composition of the binary alloy corresponding to two equilibrium phases ($\alpha + \beta$). At that chemical composition of α -phase at equilibrium corresponds to the intersection of the line T and the line $\alpha/(\alpha + \beta)$ at concentration C^α and the composition of the β -phase corresponds to the intersection of T with $\beta/(\alpha + \beta)$ at C^β . Let us imagine that we can spatially separate α - and β -phases with particles of one type at the surface and the other type resting in the bulk. If surface effects are ignored, then we obtain at a given temperature T a thermodynamically equilibrium spatially heterogeneous phase-structural state when the α -phase is mainly located at the sample surface and the β -phase is mainly in the volume, separated by an interfacing $\alpha + \beta$ two-phase region (see figure 1). This two-phase region provides mechanical adhesion of the formed phases.

In reality nobody has succeeded in achieving such a system state just after ion-beam or ion-plasma surface treatment. It is necessary to subject the system to thermal annealing which, due to diffusion and phase formation, should lead to a thermally stable spatially heterogeneous distribution of the phase-structure state.

2. Physical model and its software realization

When describing diffusion and phase formation processes in the binary lamellar metallic A–B system we used a physical model based on the following statements.

- (1) The local concentration $C_{A,B}(x, t)$ ($C_A(x, t) + C_B(x, t) = 1$) of the components A and B at the sample depth x is defined at any given moment of time t by the process of mutual diffusion of the atoms.
- (2) The partial diffusion coefficients $D_{A,B}$ of the components A and B in each other do not depend on the phase-structural state of the sample.
- (3) The rate of phase formation considerably increases the rate of diffusion.
- (4) The result of phase formation is defined by the local concentration of the components and the diagram of equilibrium states for a binary alloy:
 - if the local concentration $C(x, t)$ lies in the homogeneity region of one of the phases, $C(x, t) \in [C_{\min}, C_{\max}]_{\alpha,\beta}$, then only this phase is formed;
 - if the local concentration is in the two-phase region in the state diagram, $C(x, t) \in [C_{\min}, C_{\max}]_{\alpha+\beta}$, simultaneous formation of both phases takes place and their quantities are defined by the lever rule:

$$p^\alpha = \frac{C^\beta - C(x, t)}{C^\beta - C^\alpha}, \quad p^\beta = \frac{C(x, t) - C^\alpha}{C^\beta - C^\alpha}, \quad (1)$$

where C^α and C^β are limiting concentrations of the components in α - and β -phases, respectively.

According to the Darken phenomenological theory of mutual diffusion, diffusion of the components in a binary alloy is described by the equation [9]

$$\frac{\partial C}{\partial t} = \text{div} (D \cdot \text{grad} C), \quad (2)$$

where $C_{A,B}$ is concentrations of A and B components and D is a mutual diffusion coefficient that in the general case is a function of location and time only. Taking into account that in our case of a lamellar system the component concentrations and the mutual diffusion coefficient depend on the depth in a sample only, we get

$$\frac{\partial C(x, t)}{\partial t} = \frac{\partial}{\partial x} \left(D(x, t) \cdot \frac{\partial C(x, t)}{\partial x} \right), \quad (3)$$

$$\frac{\partial C(x, t)}{\partial t} = \frac{\partial D(x, t)}{\partial x} \cdot \frac{\partial C(x, t)}{\partial x} + D(x, t) \frac{\partial^2 C(x, t)}{\partial x^2}. \quad (4)$$

For single-phase regions (α - or β -phases) of a lamellar system, in accordance with Darken's law, the mutual diffusion coefficient in a binary alloy, provided that $C_A(x, t) + C_B(x, t) = 1$, is equal to

$$D(C_A(x, t)) = D_A C_B(x, t) + D_B C_A(x, t) = D_A(1 - C_A(x, t)) + D_B C_A(x, t). \quad (5)$$

Here $D_{A,B}$ are the partial diffusion coefficients for components A and B in each other that, in accordance with the proposed model, do not depend on the sample's phase-structural state and, therefore, do not depend on coordinate x and time t .

For the two-phase region (mixture of α - and β -phases) of a lamellar system one should take into account the presence of an interphase boundary where even in the case of thermodynamic equilibrium there is a discontinuity in component concentration from some limiting concentration in one phase (C^α) to a limiting concentration in the other one (C^β). Taking this into consideration we propose within the present physical model the mechanism of mutual diffusion in a two-phase region of a binary lamellar system.

Let us assume that mutual diffusion in this case takes place only within continuous channels formed by particles of one (α or β) phase (figure 2). Due to such diffusion the

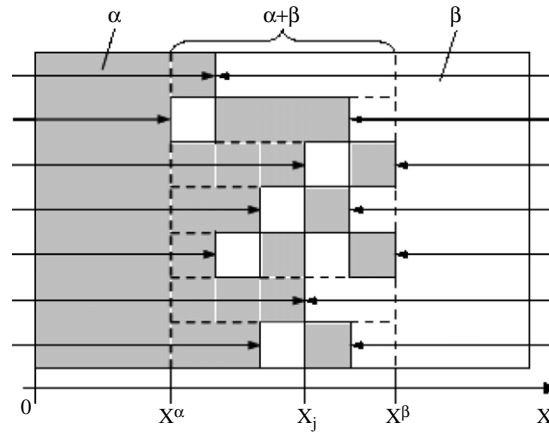


Figure 2. Schematic representation of mutual diffusion channels formed by particles of one phase in the two-phase region of a lamellar system.

condition of thermodynamic equilibrium is violated at the phase boundary and there is a redistribution of phase composition in accordance with the equilibrium state diagram.

Let particles of both phases and of the same linear size λ be generated in a two-phase region of a lamellar system. Then, in the two-phase region in the j th layer with the coordinate $x_j = x^\alpha + j \cdot \lambda$ (where x^α is the coordinate of the boundary for the one-phase region containing α -phase; see figure 2) particles of α -phase are formed with the probability p_j^α defined by the lever rule (see (1)):

$$p_j^\alpha = \frac{C^\beta - C(x_j)}{C^\beta - C^\alpha}, \quad (6)$$

where $C(x_j)$ is local concentration of the components in the j th layer.

If we assume that in different layers phase formation is independent of the phase formation in other layers, then the probability for formation of a channel from the one-phase region of α -phase to the j th layer inclusive is as follows:

$$P_j^\alpha = \prod_{i=1}^j p_i^\alpha \cdot (1 - p_{j+1}^\alpha). \quad (7)$$

Now one can calculate the probability of formation of continuous α -phase channels exceeding $x_j - x^\alpha$ in length through which mutual diffusion of the components from the one-phase region up to the j th layer take place:

$$W_j^\alpha = \sum_{i=j}^m P_i^\alpha, \quad (8)$$

where m is the number of layers in the two-phase region defined by the linear dimension of the particles and the two-phase region width: $m = \frac{x^\beta - x^\alpha}{\lambda}$ (see figure 2).

So, the effective coefficient of mutual diffusion in the two-phase region at the depth x_j , in accordance with the proposed mechanism, is defined as

$$D(x_j) = D^\alpha(x_j) + D^\beta(x_j) = (D_A(1 - C_A^\alpha) + D_B C_A^\alpha) W_j^\alpha + (D_A(1 - C_A^\beta) + D_B C_A^\beta) W_j^\beta. \quad (9)$$

Here $D^\alpha(x_j)$ and $D^\beta(x_j)$ are the coefficients of mutual diffusion of components along the channels formed by particles of α - and β -phase, respectively.

Therefore, in order to describe the diffusion and phase formation processes in a binary lamellar system one needs to solve a second-order linear differential equation in partial derivatives (4) taking into account (5) and (9) for the coefficient of mutual diffusion in different phase regions. At that, initial and boundary conditions required to solve the equation are set in accordance with specific experimental conditions.

Since we experimentally investigated lamellar systems obtained by magnetron sputtering of a binary alloy of a certain composition over the surface of a binary alloy of another composition [2–8], initial conditions were chosen in a form of a step that corresponds to the thickness of the deposited coating:

$$C(t = 0, 0 \leq x < d_{\text{coat}}) = C_{\text{coat}},$$

$$C(t = 0, d_{\text{coat}} \leq x < d = d_{\text{coat}} + d_{\text{sub}}) = C_{\text{sub}},$$

where C_{coat} , d_{coat} and C_{sub} , d_{sub} are component concentrations and thicknesses of the coating and the substrate, respectively.

In our case, the boundary conditions are defined by the absence of component flows at boundaries of the lamellar system. Since the flow of the corresponding component at some definite depth and at some definite time can be represented in the form (see (3))

$$J(x, t) = -D(x, t) \frac{\partial C(x, t)}{\partial x},$$

then, the boundary conditions are

$$\left. \frac{\partial C(t, x)}{\partial x} \right|_{x=0} = 0 \quad \text{and} \quad \left. \frac{\partial C(t, x)}{\partial x} \right|_{x=d} = 0.$$

The proposed physical model for the description of diffusion and phase formation processes in binary lamellar metallic systems has been used in our code developed within the MS Developer Studio software package with a Compaq Visual Fortran Professional Edition 6.5.0 compiler and a standard software package IVPAG/DIVPAG from the software library DIGITAL to solve the system of differential equations in partial derivatives.

Below we briefly describe the main functional features of the code.

The code envisages the presence of three one-phase and two two-phase regions in the state diagram of a binary alloy. At that, possible change in concentration boundaries for existing phases with temperature is taken into account.

Using this code one can simulate an arbitrary temperature–time regime of thermal treatment for the lamellar system under investigation including isothermal, isochronous, and combined annealing as well as take into account the terminal time taken to achieve the required temperature and cooling down. At that it is supposed that the temperature dependence for partial diffusion coefficients D_A and D_B is defined by an Arrhenius law:

$$D_{A,B}(T) = D_{A,B}^0 \cdot \exp \left\{ -\frac{Q_{A,B}}{kT} \right\}, \quad (10)$$

where $D_{A,B}^0$ and $Q_{A,B}$ are frequency factors and activation energies for the corresponding components, respectively, and k is the Boltzman constant.

With the code, at each temperature–time interval, it is possible to obtain not only local concentration of the components $C(x, t)$ upon solving equation (4), but to determine the relative phase content at any depth of the lamellar system (including the location of phase region boundaries), mutual diffusion coefficient and diffusion flow of the components.

In conclusion we list the main input parameters in the code that define the kinetics of diffusion and phase formation.

Upon the choice of the components for a lamellar binary system in accordance with equilibrium state diagram of the alloy there are set concentration boundaries of the phases (that depend in the general case on temperature) and partial diffusion coefficients $D_{A,B}$ of the components or their frequency factors $D_{A,B}^0$ and activation energies $Q_{A,B}$. For a specific sample of binary lamellar system produced by ion technologies, the concentration of the component and thicknesses of the coating ($C_{\text{coat}}, d_{\text{coat}}$) and the substrate ($C_{\text{sub}}, d_{\text{sub}}$) are set. Choice of the temperature–time regime for thermal treatment defines the settings for the array of thermal annealing temperatures at sequential time intervals. For realization of the proposed diffusion mechanism in the two-phase region of a sample it is necessary to set a characteristic linear size λ of phase particles formed in the two-phase region.

Each binary lamellar system has an equilibrium phase diagram peculiarity, various diffusion coefficients and average component concentration. In order to reveal the laws of thermally induced processes in lamellar systems we used numerical simulations; the results are presented below.

3. Comparison of theoretical calculations with experimental data

In accordance with the phase diagram for the chosen Fe–Be alloy (see, for instance [11]), within temperature intervals of interest there is a characteristic β -phase $\text{FeBe}_{2+\delta}$ and so-called higher beryllides FeBe_x including FeBe_5 . Solubility of Be in α -Fe becomes noticeable only at $\sim 250^\circ\text{C}$ and it increases considerably with temperature, achieving $\sim 29\%$ at 1000°C . In the solid phase there is almost zero solubility of Fe in Be. In the theoretical calculations, we took into account the temperature dependence of concentration boundaries for co-existing phases in the Fe–Be binary alloy.

Setting of temperature values for thermal annealing at successive time intervals made it possible to take into account the real temperature–time regime for thermal processing of a specific lamellar Fe–Be system. We simulated successive isochronous and isothermal temperature–time regimes for the thermal treatment of lamellar systems under investigation and took into account the lengths of time to reach a given annealing temperature (~ 1 h) and to cool down (~ 0.3 h).

The partial coefficients for diffusion of iron and beryllium and vice versa required for the theoretical description of thermally induced processes were obtained on the basis of [12–14]. In accordance with these data, for both components in bulk samples, the Arrhenius law (10) is true. We chose the following values of frequency factors and activation energies for the two components: $D_{\text{Fe}}^0 = 1 \text{ cm}^2 \text{ s}^{-1}$, $Q_{\text{Fe}} = 220 \text{ kJ mol}^{-1}$ [12, 13] and $D_{\text{Be}}^0 = 0.1 \text{ cm}^2 \text{ s}^{-1}$, $Q_{\text{Be}} = 241.2 \text{ kJ mol}^{-1}$ [14]. Since during magnetron sputtering of beryllium over α -Fe substrate there usually appears a column coating structure [15], we considered the possibility of atom diffusion through grain boundaries. The partial coefficients of Fe atom diffusion into Be were varied and in some cases exceeded the values obtained on the basis of literature data by one or even two orders of magnitude (see below).

For incorporation of the proposed diffusion mechanism in the two-phase region, a characteristic linear size λ of the phase particles was taken to be, in the case of Fe–Be binary alloy, $0.05 \mu\text{m}$.

When comparing calculation results with Mössbauer spectroscopy data, it was supposed that the Mössbauer effect probabilities for Mössbauer atoms in different phases (intermetallides and solutions) of a binary alloy are close. In this case, the relative intensities of the partial spectra obtained by registration of γ -quanta in transition geometry (MS-spectra) are equal to the relative concentrations of Fe atoms belonging to different phases; the code includes their calculations.

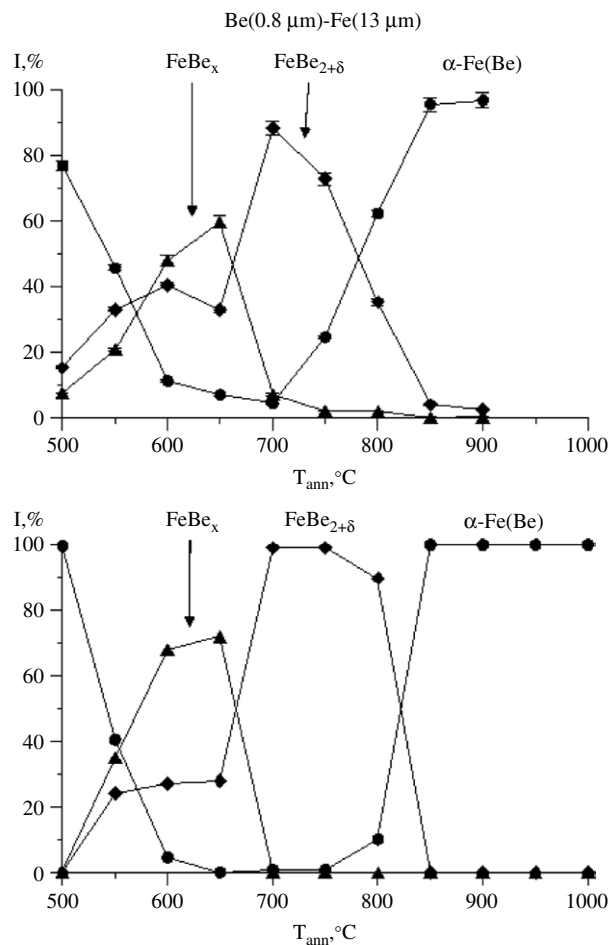


Figure 3. Experimental and calculated relative intensities I of partial CEMS-spectra for the lamellar Be(0.8 μm)–Fe(13 μm) system versus time of successive isothermal annealing t_{ann} .

In order to calculate the relative intensities of the partial spectra obtained by registration of conversion electrons in back-scattering geometry (CEMS-spectra), one should take into account the yield function $F(x)$ of registered conversion electrons. In our case, the yield function depends on the concentration profiles along the sample depth for both atoms A ($C_A(x)$) and atoms B ($C_B(x)$) undergoing changes during thermal annealing. We accepted this function in exponential form:

$$F(x) = \exp\left(-\frac{\int_0^x C_A(x) dx}{h_A}\right) \cdot \exp\left(-\frac{\int_0^x C_B(x) dx}{h_B}\right),$$

where h_A and h_B are the effective registration depths for conversion electrons in homogeneous layers from A and B components, respectively. To calculate the relative intensities of the partial spectra from the registration of conversion electrons in back-scattering geometry, we made theoretical and experimental assessments of the effective registration depths for conversion electrons [3]. So, for a description of the experimentally observed dependency of relative phase intensities for lamellar Fe–Be systems, the values of $h_{\text{Fe}} = 0.04 \mu\text{m}$ and $h_{\text{Be}} = 1 \mu\text{m}$ were chosen.

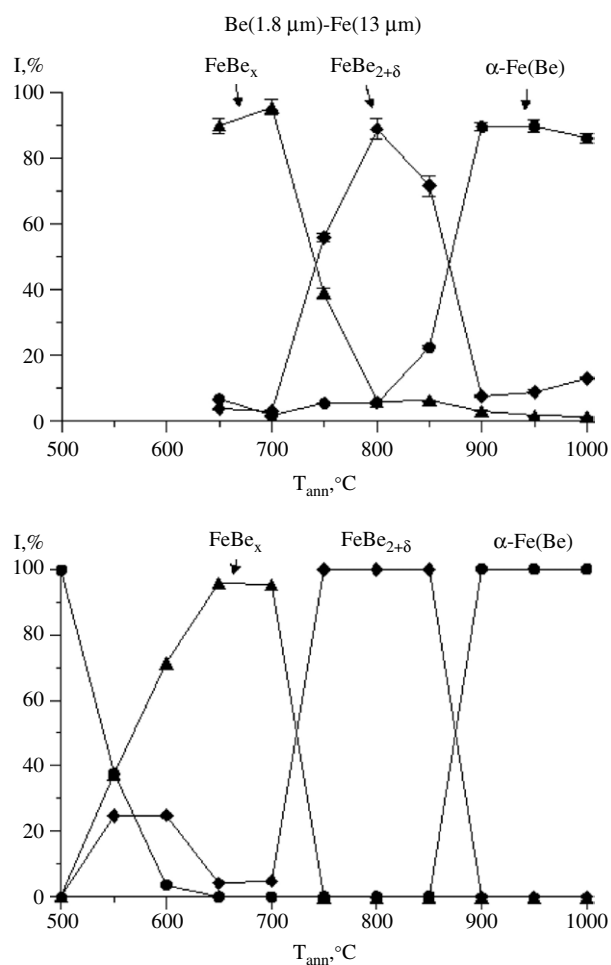


Figure 4. Experimental and calculated relative intensities I of partial CEMS-spectra for the lamellar Be(1.8 μm)–Fe(13 μm) system versus time of successive isothermal annealing t_{ann} .

Let us note that MS-spectra include information about a lamellar system as a whole while CEMS-spectra provide information regarding the surface layers. For the Fe–Be lamellar system, the thickness of these surface layers is about 0.3 μm .

First, we present below the results of diffusion and phase transformation processes in lamellar Fe–Be systems at isochronous annealing obtained by the method of Mössbauer spectroscopy when the average beryllium concentration did not exceed the limit of its solubility in iron. Figures 3 and 4 present the relative intensities I of CEMS-spectra of lamellar Be(0.8 μm)–Fe(13 μm) and Be(1.8 μm)–Fe(13 μm) systems versus the terminal temperature of successive isochronous annealing T_{ann} . One can see that the experimental dependence is of a complex nature that corresponds to successive mutual transformations of phases.

Some peculiarities of the observed phase formation processes are to be mentioned. The investigated temperature interval T_{ann} can be conditionally divided into three regions (see figure 3): low temperatures ($T_{\text{ann}} \leq 600^\circ\text{C}$) when beryllides are conceived; moderate temperatures ($600^\circ\text{C} < T_{\text{ann}} < 750\text{--}850^\circ\text{C}$) when the formed beryllides ‘compete’ with

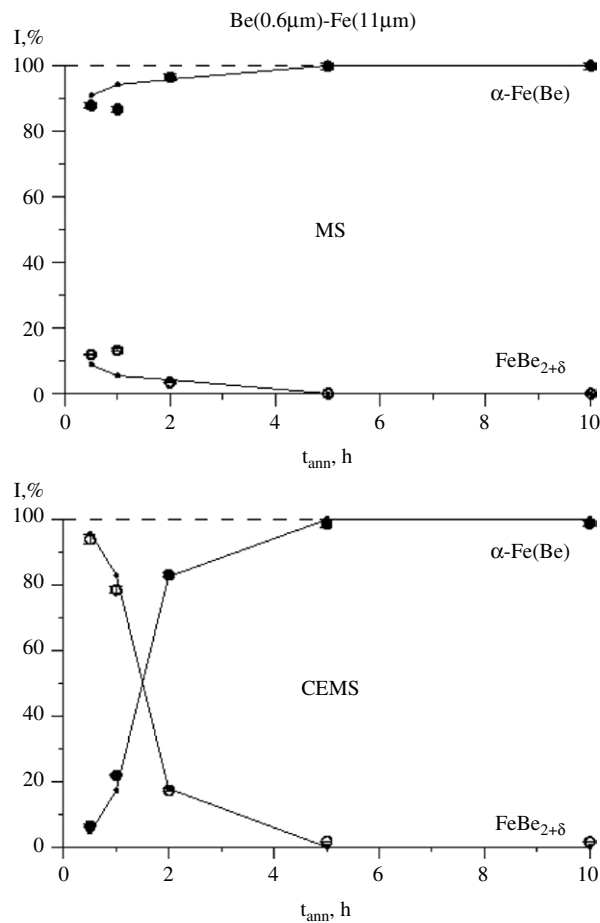


Figure 5. Relative intensities I of partial MS- and CEMS-spectra for the lamellar Be(0.6 μm)–Fe(11 μm) system versus time of successive isothermal annealing t_{ann} . Circles denote experimental data, and points, connected by solid lines, are calculation results.

each other; and high temperatures ($T_{ann} > 750\text{--}850\text{ }^\circ\text{C}$) when the formed beryllides undergo decomposition and Be atoms come to the solution $\alpha\text{-Fe(Be)}$. The kinetics of phase formation at temperatures $T_{ann} \leq 600\text{ }^\circ\text{C}$ does not practically depend on the thickness of the deposited coating. At $600\text{ }^\circ\text{C}$, the thickness of dissolved beryllium at the iron-facing side is about $0.5\text{ }\mu\text{m}$.

For larger coating thickness (figure 4), the main characteristic processes of phase transformations ('competition' and decomposition of beryllides) take place at higher annealing temperatures, which is quite as expected due to the additional 'replenishment' of Be atoms from the surface of the diffusion layer.

In these figures, calculated curves for the intensities of the partial spectra for different phases versus temperature of isochronous annealing obtained using the physical model described above are given. One can see that all the main peculiarities of the partial spectra relative intensity change and, correspondingly, the proportions of different phases in surface layers of the investigated systems are well described by the theory with increase of annealing temperature. The best agreement is achieved with an increase (compared to bulk samples) of the frequency factor for Fe atoms of 3 times in the case of the lamellar Be(0.8 μm)–Fe(13 μm)

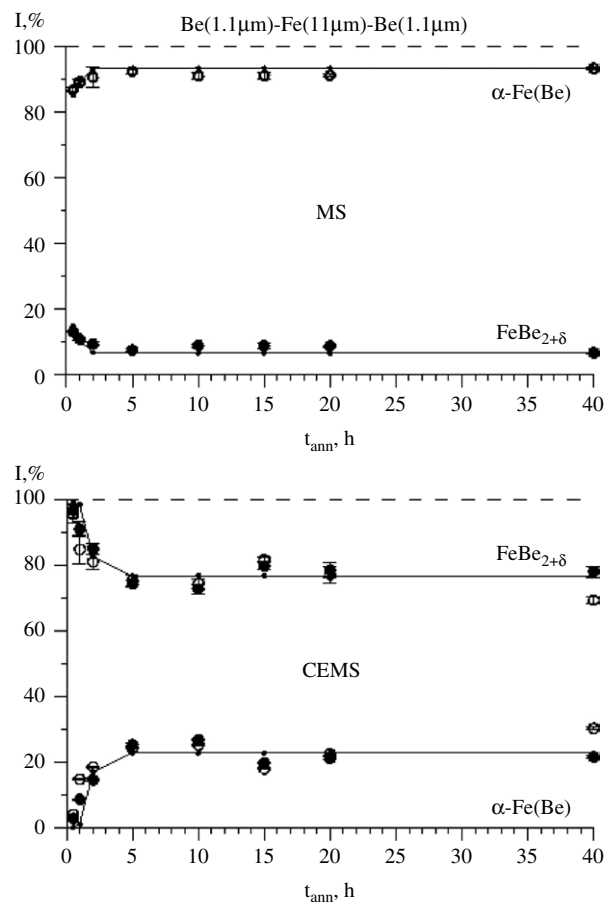


Figure 6. Relative intensities I of partial MS- and CEMS-spectra for the lamellar Be(1.0 μm)–Fe(11 μm)–Be(1.2 μm) system versus time of successive isothermal annealing t_{ann} . Circles denote experimental data, and points, connected by solid lines, are calculation results. For the CEMS data, filled and open circles represent experimental data for the Be(1.0 μm) and Be(1.2 μm) sides of the samples, respectively.

system and of 3.5 times in the Be(1.8 μm)–Fe(13 μm) system. At that, the frequency factor for Be atoms and activation energies for both components were equal to the values for bulk samples.

Let us now compare the theoretical calculations with experimental data [4, 5] obtained from successive isothermal annealing of lamellar Fe–Be systems where the average beryllium concentration does not exceed in the two-layer Be(0.6 μm)–Fe(11 μm) system and does exceed in the three-layer Be(1.0 μm)–Fe(11 μm)–Be(1.2 μm) system its solubility limit in iron.

The experimental (denoted with circles) and calculated (points) dependences of the relative intensities I of the partial CEMS-spectra of ^{57}Fe on time of isothermal annealing at 710 $^{\circ}\text{C}$ for the lamellar Be(0.6 μm)–Fe(11 μm) system are presented in figure 5. In the figure one can see that the calculated curve obtained taking into account time for reaching the annealing temperature and cooling down agrees well with the observed experimental data. For short annealing times, there is mainly β -beryllide FeBe_{2+δ} in a surface layer on the side previously coated with Be (see the relative intensities of the partial CEMS-spectra in figure 5) and then,

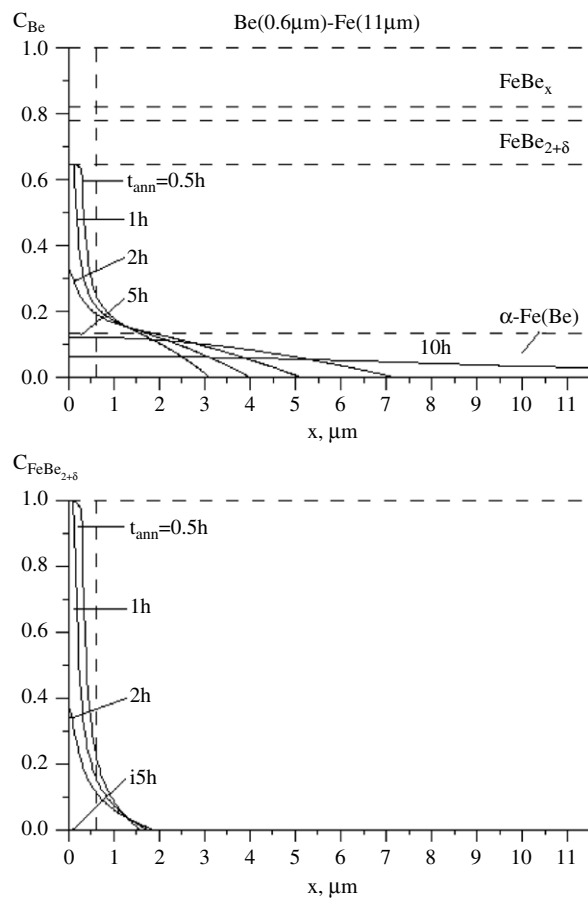


Figure 7. Beryllium concentration C_{Be} and relative content of $C_{FeBe_{2+\delta}}$ of phase $FeBe_{2+\delta}$ (in amu Fe) for the lamellar $Be(0.6 \mu m)-Fe(11 \mu m)$ system as a function of distance x to the sample surface for different times of successive isothermal annealing t_{ann} . The horizontal dashed lines denote concentration regions of existing phases and the vertical dashed lines denote coating thickness.

with increased annealing time, the relative intensity of the partial spectrum from $FeBe_{2+\delta}$ becomes lower. In other words, there is decomposition of β -beryllide in the surface layer accompanied with increase of beryllium concentration in the solution $\alpha-Fe(Be)$ [4, 5]. For better agreement of calculation results and experimental data, the frequency factor for Fe atom was increased to 17 times that used for the bulk sample. Some lower values obtained in experimental data on relative intensities of MS-spectra for $\alpha-Fe(Be)$ -phase in comparison with calculated ones (see figure 5) can be explained by 'saturation' (see, for instance [16]).

Figure 6 presents the experimental (circles) dependence for relative intensities I of CEMS-spectra for the three-layer lamellar $Be(1.0 \mu m)-Fe(11 \mu m)-Be(1.2 \mu m)$ system versus time of successive isothermal annealing t_{ann} at $720^\circ C$. One can see that, for short annealing times, in the surface layer there appears mainly beryllide $FeBe_{2+\delta}$ from the Be-coated side. Increase in annealing time results in some decrease in intensity of the partial spectrum $FeBe_{2+\delta}$, i.e. there is decomposition of β -beryllide in this subsurface layer as in case of the two-layer system. Nevertheless, at $t_{ann} \geq 5$ h there is thermal stability of the β -beryllide and the solution $\alpha-Fe(Be)$ in the investigated three-layer system. That means that all phase formation processes

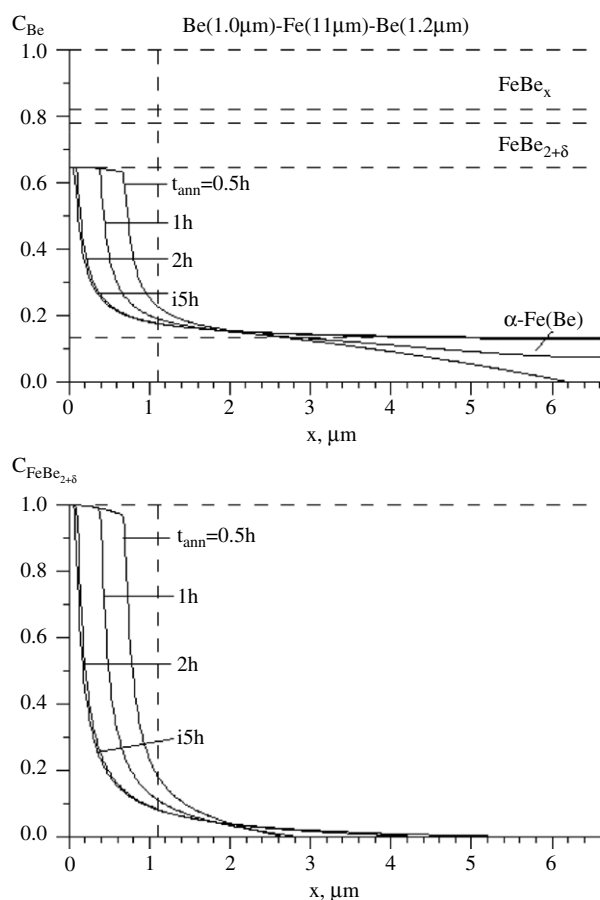


Figure 8. Beryllium concentration C_{Be} and relative content of $C_{FeBe_{2+\delta}}$ of phase $FeBe_{2+\delta}$ (in amu Fe) in the lamellar $Be(1.0\ \mu m)-Fe(11\ \mu m)-Be(1.2\ \mu m)$ system as a function of distance x to the sample surface for different times of successive isothermal annealing t_{ann} . The horizontal dashed lines denote concentration regions of existing phases and the vertical dashed lines denote coating thickness.

within the entire sample bulk have stopped [4, 5]. At that the phase $FeBe_{2+\delta}$ contributes to ~ 78 at.% Fe in the surface layer and ~ 8 at.% Fe within the whole sample volume [5].

Points on the same figure present the calculated intensities of partial CEMS-spectra for various phases of a three-layer lamellar system versus time of successive isothermal annealing t_{ann} obtained using the proposed physical model. One can see (figure 6) that the calculated points obtained, as in the case of the two-layer system, taking into account the time to reach the annealing temperature and time for cooling down, describe the experimental data well, including the observed process of thermal stabilization. For better agreement of calculated results and experimental data, the frequency factor for the Fe atom was increased in this case to 75 times that for the bulk sample. Such an increase of the frequency factor seems to be related to the considerable difference in the structures of the Be-coating layer (grains, column structure, etc) and bulk Be [15]; at that, higher diffusion rates for Fe atoms in the sputtered Be-layer is possible.

It follows from the comparison of calculated and experimental data that the proposed physical model adequately describes the diffusion and phase transformation processes in

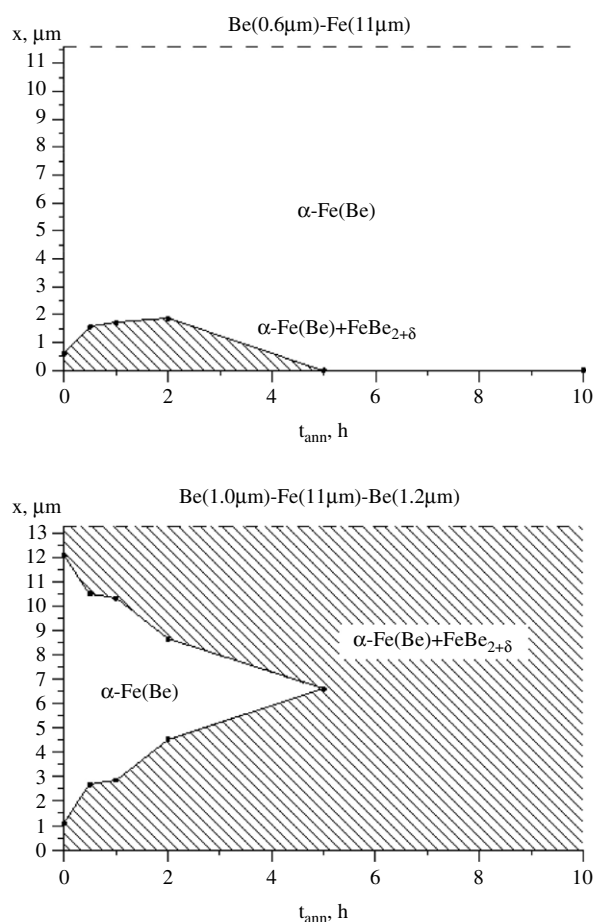


Figure 9. Location of boundary between two-phase region $\alpha\text{-Fe(Be)} + \text{FeBe}_{2+\delta}$ and solution $\alpha\text{-Fe(Be)}$ in the lamellar Be(0.6 μm)–Fe(11 μm) system and in the lamellar Be(1.0 μm)–Fe(11 μm)–Be(1.2 μm) system depending on time of successive isothermal annealing t_{ann} (calculation results).

the investigated systems, strongly suggesting the validity of intermediate calculations of concentration profiles for components and phases, boundaries of phase regions, local coefficients of mutual diffusion, etc.

The code makes it possible to obtain not only the local concentration of components $C(x, t)$ as a solution of the differential equation (1), but to determine the relative phase content at any depth of a lamellar system (for instance, the location of phase region boundaries) as well as the mutual diffusion coefficient, flow and chemical potentials of components for each temperature–time interval.

For comparison, figures 7 and 8 present the calculated concentration profiles for Be atoms and formed phase of β -beryllide $\text{FeBe}_{2+\delta}$ at different stages of successive isothermal annealing for two-layer and three-layer systems. It is seen that in the first case complete dissolution of Be atoms in $\alpha\text{-Fe}$ takes place and in the second, a spatially heterogeneous distribution of the phase-structural state is formed. The thickness of the surface layer that includes mainly β -beryllide $\text{FeBe}_{2+\delta}$ (>80 at.% Fe) is $\sim 0.1 \mu\text{m}$. It should be noted that in the last case the entire sample becomes a two-phase structure due to thermal stabilization.

Figure 9 presents for comparison the calculation results for boundary positions between the two-phase regions α -Fe(Be) + FeBe_{2+ δ} and the solution α -Fe(Be) in the two-layer Be(0.6 μ m)–Fe(11 μ m) and the three-layer Be(1.0 μ m)–Fe(11 μ m)–Be(1.2 μ m) systems at various stages of consecutive isothermal annealing. One can see that in the first case a complete dissolution of Be atoms in α -Fe is observed; in the second case, a spatially heterogeneous distribution of the phase-structural state in the sample depth is formed. It should be noted that in the second case the whole sample becomes a two-phase one due to thermal stabilization.

4. Conclusions

A physical model has been proposed for thermally induced processes in binary lamellar systems that describes diffusion, phase formation and thermal stabilization of the spatially heterogeneous phase-structural state of the systems. The model is based on Darken's theory of mutual diffusion with the assumption that the phase-formation rate greatly exceeds the diffusion one; it is also based on the proposed mutual diffusion mechanism for two-phase concentration regions.

A computer code has been made that describes quantitatively the kinetics of such processes in any region of lamellar systems for any given annealing regime. For comparison with experimental data, the relative intensities of Mössbauer spectra obtained both at γ -quantum registration in transition geometry and at registration of conversion electrons in back-scattering geometry have been calculated.

Good agreement of theoretical calculations with Mössbauer investigations of lamellar Fe–Be systems subjected to subsequent thermal annealing has been achieved.

References

- [1] Kadyrzhanov K K, Turkebaev T E and Udovsky A L 1995 *Nucl. Instrum. Methods B* **103** 38
- [2] Kadyrzhanov K K, Rusakov V S and Turkebaev T E 2001 *Izv. Ross. Akad. Nauk, Ser. Fiz.* **65** 1022 (in Russian)
- [3] Kadyrzhanov K K, Rusakov V S, Turkebaev T E, Kerimov E A and Lopuga A D 2001 *Nucl. Instrum. Methods B* **174** 463
- [4] Kadyrzhanov K K, Rusakov V S, Turkebaev T E, Kerimov E A and Plaksin D A 2002 *Hyperfine Interact.* **141/142** 453
- [5] Kadyrzhanov K K, Kerimov E A, Plaksin D A, Rusakov V S and Turkebaev T E 2003 *Poverchnost* (8) 74 (in Russian)
- [6] Kadyrzhanov K K, Rusakov V S, Korshiev B O, Turkebaev T E and Vereschak M F 2004 *Hyperfine Interact.* **156/157** 623
- [7] Rusakov V S, Kadyrzhanov K K, Suslov E E, Plaksin D A and Turkebaev T E 2004 *Poverchnost* (12) 22 (in Russian)
- [8] Rusakov V S, Kadyrzhanov K K, Korshiev B O, Turkebaev T E and Vereschak M F 2005 *Poverchnost* (1) 60 (in Russian)
- [9] Gurov K P, Kartashkin B A and Ugaste Yu E 1981 *Mutual Diffusion in Many-Phase Metal Systems* (Moscow: Nauka) p 350 (in Russian)
- [10] Cahn R W and Haasen P (ed) 1983 *Physical Metallurgy* vol 2 (Amsterdam: North-Holland) p 610
- [11] Kubashevsky O 1985 *State Diagrams for Binary Iron-based Systems* (Moscow: Metallurgiya) p 182 (in Russian)
- [12] Donze G *et al* 1962 *C. R. Acad. Sci.* **254** 2328
- [13] Naik M C and Dupony J M 1966 *Mem. Sci. Rev. Metall.* **63** 488
- [14] Grigoriev G V and Pavlinov L V 1968 *Pyz. Metall. Mater.* **25** 836 (in Russian)
- [15] Tuleushev A Zh, Lisitsyn V N, Volodin V N and Tuleushev Yu Zh 2002 *Bull. NNC RK* **4** 26 (in Russian)
- [16] Nikolaev V I and Rusakov V S 1985 *Mössbauer Investigation of Ferrites* (Moscow: Moscow State University) p 224 (in Russian)